

## Link between Adatom Resonances and the Cu(111) Shockley Surface State

Jérôme Lagoute, Xi Liu, and Stefan Fölsch

*Paul-Drude-Institut für Festkörperelektronik, Hausvogteiplatz 5-7, D-10117 Berlin, Germany*

(Received 28 June 2005; published 19 September 2005)

Low-temperature scanning tunneling microscopy and spectroscopy at 7 K was used to assemble and characterize native adatom islands of successive size on the Cu(111) surface. Starting from the single adatom we observe the formation of a series of quantum states which merge into the well known two-dimensional Shockley surface state in the limit of large islands. Our experiments reveal a natural physical link between this fundamental surface property and the  $sp_z$  hybrid resonance associated with the single Cu/Cu(111) adatom.

DOI: [10.1103/PhysRevLett.95.136801](https://doi.org/10.1103/PhysRevLett.95.136801)

PACS numbers: 73.20.At, 68.37.Ef, 68.47.De, 81.16.Ta

Atomic clusters are the subject of extensive research because they bridge the state of quasimolecular coordination and the state of condensed matter. There is a great deal of interest in size-specific cluster properties induced by coordination and confinement effects. In transition metals, for example, such effects lead to new electronic, magnetic, and catalytic properties [1–3]. From the fundamental point of view, clusters comprised of only a few atoms provide an ideal model case to explore how electronic properties evolve with size. The low-temperature scanning tunneling microscope (LT-STM) offers the unique possibility to build up surface-supported model structures atom by atom [4,5] and—at the same time—to characterize their local electronic properties by  $dI/dV$  spectroscopy [6]. This technique was recently applied to construct monatomic Au/NiAl(110) [7] as well as Cu/Cu(111) adatom chains [8] and to explore the electron dynamics in these quasi-one-dimensional (1D) objects.

Here, experimental evidence is provided on how the two-dimensional (2D) Shockley surface state evolves from quasiautomatic resonances associated with single adatoms. In detail, we study the electronic structure of native adatom islands of successive size assembled by atomic manipulation on the Cu(111) surface. Starting from the discrete Cu adatom we observe the formation of a series of quantum states which merge into the Shockley surface state in the limit of large islands. For the first time, the physical linkage between this archetype electronic surface property and its atomic counterpart is identified and characterized. Our findings suggest that adatom resonances and quantum confinement in compact adatom structures are inherent to a variety of other one-component metal systems.

The experiments were performed with a home-built LT-STM operated at 7 K. The Cu(111) surface was prepared by standard procedures in ultrahigh vacuum as described in Ref. [8]. Single Cu adatoms were created by controlled tip-surface contact at 7 K. The tungsten tip was dipped  $\sim 5$  to  $6$  Å into the surface and subsequently retracted to a tip height of  $\sim 6$  Å while applying a voltage of  $-4$  to  $-5$  V to the tip-sample junction (voltage referring to the sample with respect to the tip). In this way, adatoms and clusters

are created which are dispersed over the surface close to the contact area. Only native adatoms are formed by this procedure [as evident from their spectroscopic signature [9]] which is in line with previous work [10] on  $W$  tip-induced adatom formation on Ag(111). By reducing the tip height to  $\sim 1.5$  Å, single adatoms can be manipulated along arbitrary lateral directions at a tunneling resistance of  $\sim 0.1$  M $\Omega$ .

The top left panel in Fig. 1 shows constant-current images (1 nA, 50 mV,  $32$  Å  $\times$   $16$  Å) of compact triangular Cu islands assembled from six [Fig. 1(b)], ten [Fig. 1(c)], and 15 Cu atoms [Fig. 1(d)] by lateral manipulation (the horizontal direction is parallel to the in-plane close-packed row direction along  $[1\bar{1}0]$ ). The apparent height of these islands increases from  $1.5$  Å for Cu<sub>6</sub> and  $1.8$  Å for Cu<sub>10</sub> to  $1.9$  Å for Cu<sub>15</sub> at the present sample bias [the monatomic step height of Cu(111) is  $2.08$  Å]. We interpret the regular triangular shape together with the observed lateral and vertical dimensions as a clear indication that the Cu atoms within the island reside on substrate lattice sites and adopt a close-packed arrangement; the hexagonal atomic structure is indicated by white dots in Figs. 1(b)–1(d).

The close-packed Cu trimer shown in Fig. 1(a) is imaged as a protrusion of almost isotropic shape with a height of  $1.2$  Å and a half width of  $\sim 7.7$  Å. We find that this structure cannot be formed directly by lateral manipulation at a temperature of 7 K: joining a single adatom and a dimer always yields a linear trimer which is readily identifiable by its length of  $10.1$  Å and peaks in the  $dI/dV$  spectra at  $2.00$  V and  $3.50$  V [8]. We attribute this behavior to (i) the fact that the Cu dimer diffuses locally at temperatures  $>5$  K within a cell of hollow sites centered around an on-top site [11] and (ii) an anisotropic repulsive adatom-dimer interaction revealed by density functional theory (DFT) calculations which makes it harder for an adatom to approach the dimer in the middle than at the ends [12]. Nonetheless, close-packed trimers are frequently formed (among monomers, dimers, linear trimers, and larger clusters) during the tip-surface contact procedure. Though direct atom counting during assembly cannot be performed here, we find that the close-packed trimer

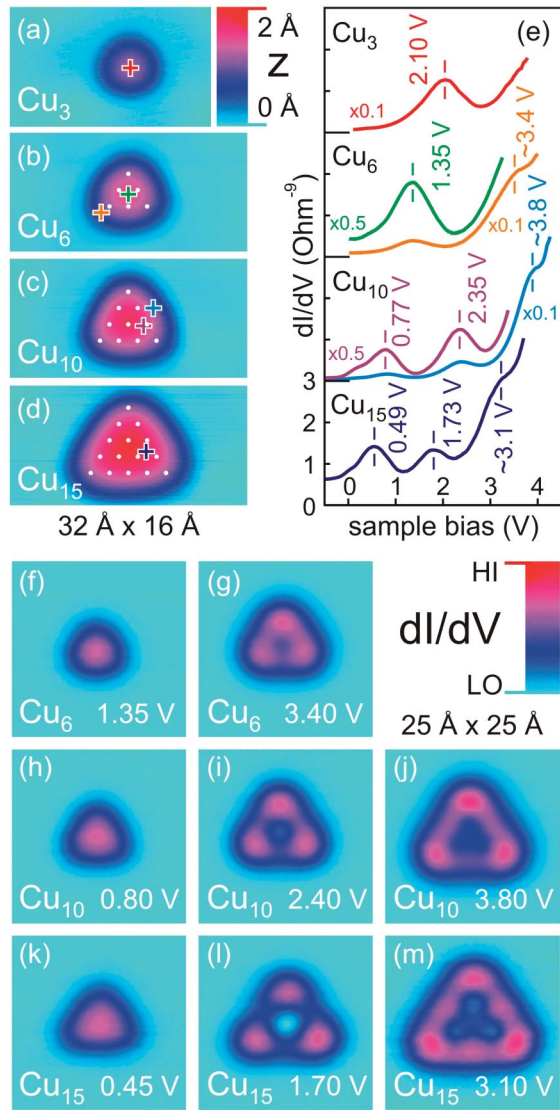


FIG. 1 (color). Top left panel: constant-current images (1 nA, 50 mV,  $32 \text{ \AA} \times 16 \text{ \AA}$ , 7 K) of a close-packed Cu trimer (a) and triangular islands assembled from six (b), ten (c), and 15 Cu atoms (d); atomic positions are indicated by white dots in (b), (c), and (d). Top right panel, (e)  $dI/dV$  spectra of the trimer (red), the Cu<sub>6</sub> (green/orange), the Cu<sub>10</sub> (magenta/blue), and the Cu<sub>15</sub> island (dark blue) measured at constant tip height [respective tip positions as indicated by crosses in (a)–(d)]; for clarity, spectra are offset by a constant of  $3 \times 10^{-9} \text{ \Omega}^{-1}$ , relative to the lowest curve. Lower panel, (f)–(m) corresponding  $dI/dV$  maps ( $25 \text{ \AA} \times 25 \text{ \AA}$ ) indicate the spatial variation of the state density at energies at which peaks in the  $dI/dV$  spectra [cf. (e)] are observed. Tunneling parameters prior to turning off the feedback loop: 1 V, 1 nA; amplitude and frequency of the lock-in modulation: 50 mV, 650 Hz.

tends to irreversibly transform into a linear trimer when injecting electrons at biases  $>3.5 \text{ V}$  and currents of  $\sim 20 \text{ nA}$ , thus corroborating that the structure consists of three Cu atoms.

Figure 1(e) shows  $dI/dV$  spectra as a measure of the local density of states (LDOS) recorded at constant tip

height with the tip located at the positions indicated by crosses in Figs. 1(a)–1(d). The close-packed trimer exhibits a single resonance at 2.10 V (red curve) whereas a pronounced peak at 1.35 V and a shoulder at  $\sim 3.4 \text{ V}$  are found for the Cu<sub>6</sub> island (green and orange). This observation shows—in line with our previous studies on Cu adatom chains [8]—that compact structures comprised of native adatoms on Cu(111) exhibit unoccupied quantum states in the pseudogap [13] of the projected bulk bands. These quantum states arise from the coupling between  $sp_z$  hybrid adatom states [9] associated with a resonance  $\sim 3.3 \text{ eV}$  above the Fermi level  $E_F$ . Consistently, when further increasing the size of the triangular quantum dot the levels shift downwards in energy and their separation decreases. This is evident from the  $dI/dV$  spectra in Fig. 1(e) obtained for a Cu<sub>10</sub> (magenta and blue) and a Cu<sub>15</sub> island (dark blue) [14]. We measured the spatial variation of the quantum states by mapping the  $dI/dV$  signal at constant tip height and at biases at which peaks in the  $dI/dV$  spectra are observed [cf. Figs. 1(f)–1(m)]. Clearly, the ground state of the Cu<sub>6</sub> [Fig. 1(f)], the Cu<sub>10</sub> [Fig. 1(h)], and the Cu<sub>15</sub> island [Fig. 1(k)] is composed of a single lobe while for the first excited state [cf. Figs. 1(g), 1(i), and 1(l)] the squared wave function amplitude is centered close to the corners of the triangle. Finally, the maps of the Cu<sub>10</sub> [Fig. 1(j)] and the Cu<sub>15</sub> island [Fig. 1(m)] corresponding to the high-energy peak in the  $dI/dV$  spectra are more complex showing a LDOS distribution which is peaked at the corners and nonzero along the sides of the structure.

In the following it is shown that the tight-binding (TB) approximation is capable of describing the confinement behavior in atomic-scale 2D Cu/Cu(111) islands. We find that there is a natural link between the  $sp_z$  hybrid state associated with the discrete adatom, the quantum state confinement in compact adatom structures, and the well established 2D Shockley surface state of the extended Cu(111) surface. We previously reported that the dispersion of quantum states in monatomic Cu/Cu(111) chains is well approximated by a 1D TB band  $\varepsilon(k) = \alpha - 2\gamma \cos(ka)$  centered at an energy position  $\alpha$  close to the adatom resonance with a band width of  $4\gamma = 3.6 \text{ eV}$  [8] (the TB parameter  $\alpha$  is associated with the Coulomb integral and the hopping integral  $\gamma = 0.9 \text{ eV}$  describes the nearest-neighbor coupling). Turning now to the case of a hexagonal triangular 2D island comprised of  $N$  atoms, we start with the  $N \times N$  secular determinant describing the problem within the simple Hückel scheme [15]: all diagonal elements are given by  $\alpha - \varepsilon_i$  with the eigenvalues  $\varepsilon_i$ , off-diagonal elements between neighboring atoms are  $\gamma$ , and all other elements are zero. We thus treat the island as an artificial molecule with all  $\alpha$  values set equal; i.e., all atoms are treated identically. Note that the nearest-neighbor coupling, which is described by the quantity  $\gamma$  within this simple parametrization, includes contributions both of direct interatomic coupling as well as of substrate-mediated coupling [16]. Numerical solution of the secular determinant of an equilateral triangular island comprised

of, e.g., six atoms, gives the eigenvalues  $\varepsilon_0 = \alpha - 3.236\gamma$  as the ground state energy and  $\varepsilon_1 = \alpha - 0.618\gamma$  as the energy of the first excited state (the latter eigenvalue is doubly degenerated within the TB model). With the experimental values  $\varepsilon_0 = 1.35$  eV and  $\varepsilon_1 \cong 3.4$  eV [cf. Fig. 1(e)] these two expressions yield  $\alpha = 3.87$  eV and  $\gamma = 0.78$  eV for the  $\text{Cu}_6$  island. Similar  $\alpha$  and  $\gamma$  values are obtained for the larger islands, namely, 3.75 eV and 0.74 eV for  $N = 10$ , and 3.76 eV and 0.73 eV for  $N = 15$ . As a first test of consistency, we calculate the energies of higher excited states from the respective eigenvalue expressions and the corresponding  $\alpha$  and  $\gamma$  values: for the second and third excited state one gets  $\varepsilon_{2(3)} = 3.75(4.00)$  eV for  $N = 10$  and  $\varepsilon_{2(3)} = 2.95(3.17)$  eV for  $N = 15$ . These energies compare well with the high-energy shoulders in the spectra of the  $\text{Cu}_{10}$  and the  $\text{Cu}_{15}$  island at  $\sim 3.8$  V and  $\sim 3.1$  V, respectively, suggesting that the LDOS distributions in Figs. 1(j) and 1(m) correspond to the superposition of two resonance-broadened states each.

To verify a superposition of states we calculated the squared wave function amplitude of the four lowest eigenstates of the triangular  $\text{Cu}_{15}$  island within the TB framework. The linear-combination-of-atomic-orbitals coefficients were extracted from the secular determinant and  $s$ -like radial orbital character was chosen to model the decay of the atomic orbitals centered at the respective lattice sites within the structure. To determine a realistic value of the decay constant, we measured the adatom resonance peak at  $\sim 3.3$  V as a function of the tip-to-surface separation ranging from 9 to 11 Å and find that the  $dI/dV$  peak magnitude decays exponentially with a decay constant of  $1.66 \text{ \AA}^{-1}$ . Regarding that the differential tunneling conductance provides a measure of the squared wave function [6] the decay constant accounting for the wave function vacuum tail was set to  $0.83 \text{ \AA}^{-1}$ .

Figure 2 shows false color plots of the calculated squared wave function amplitude  $|\Psi|^2$  of the four lowest states [cf. Figs. 2(a)–2(d)]. The  $|\Psi|^2$  maps refer to a constant height of 4 Å above the structure to match the experimental tip height (the atomic positions are indicated by dots). Comparison of the ground state and the first excited state  $|\Psi|^2$  maps in Figs. 2(a) and 2(b) with their experimental counterparts in Figs. 1(k) and 1(l) yields good agreement. Figure 2(e) shows a superposition of the squared wave function amplitudes of the second [Fig. 2(c)] and the third excited state [Fig. 2(d)] at an energy of 3.1 eV assuming a resonance broadening of  $\sim 0.6$  eV [17]. As evident, overall agreement with the experimental LDOS map in Fig. 1(m) measured at a sample bias of 3.1 V is also obtained in this case. We interpret this finding as a further indication that TB provides an adequate modeling of the system.

Figure 3 summarizes the size-dependent experimental energies of the ground state (circles), the first excited state (squares), and the high-energy shoulder (triangles) extracted from the  $dI/dV$  spectra in Fig. 1(e). Crosses

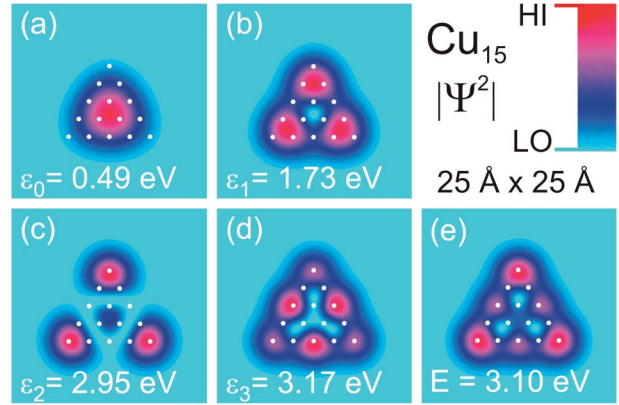


FIG. 2 (color). Maps of the calculated squared wave function amplitude [ $25 \text{ \AA} \times 25 \text{ \AA}$ , (a)–(d)] of the four lowest states of the  $\text{Cu}_{15}$  island at the respective energies  $\varepsilon_i$ ; the map in (e) represents the superposition of the squared wave function amplitudes of the resonance-broadened second (c) and the third excited state (d) at an energy of 3.1 eV and compares well with the measured counterpart in Fig. 1(m). Atomic positions are indicated by white dots (see text for details on the TB calculation).

mark corresponding energies of the four lowest states calculated with  $\alpha = 3.76$  eV and  $\gamma = 0.73$  eV as obtained for the largest assembled island with  $N = 15$  (the inset details the parameter variation with  $N$ ). The TB dispersion of an infinitely large 2D island (equivalent to a hexagonal

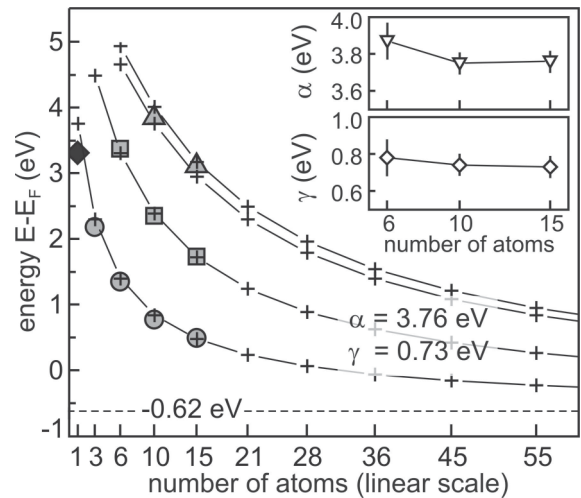


FIG. 3. Measured energies [cf. Fig. 1(e)] of the ground state (circles), the first excited state (squares), and the high-energy shoulder (triangles) as a function of the number  $N$  of atoms in the island; the energy of the adatom resonance is also indicated (black diamond). For comparison, energies of the four lowest states calculated with  $\alpha = 3.76$  eV and  $\gamma = 0.73$  eV are marked by crosses. Inset: variation of the TB parameters  $\alpha$  and  $\gamma$  with the island size expressed by  $N$ ; error bars result from estimated uncertainties of the experimental energy values extracted from the  $dI/dV$  spectra. The dashed line at  $-0.62$  eV marks the bottom of the TB energy band of a hexagonal 2D lattice with the intrinsic Cu-Cu spacing  $a = 2.55 \text{ \AA}$  and the  $\alpha$  and  $\gamma$  values as indicated.

2D lattice described by the effective parameters  $\alpha$  and  $\gamma$ ) is  $\varepsilon(\mathbf{k}) = \alpha - 2\gamma[\cos(k_x a) + 2\cos(k_x a/2) \times \cos(k_y a\sqrt{3}/4)]$ ;  $k_x$  and  $k_y$  denote the orthogonal wave vector components with  $\hat{\mathbf{e}}_x$  pointing along a close-packed row direction and  $a = 2.55 \text{ \AA}$  is the interatomic spacing. From this relation we obtain a lower band edge of  $\alpha - 6\gamma = -0.62 \text{ eV}$  and an effective mass of  $m_{x,y}^* = \hbar^2/(3\gamma a^2) = 0.53m_e$ . Regarding the simplicity of this description as well as potential size-dependent effects, the correspondence to the Cu(111) Shockley surface state onset at  $-0.44 \text{ eV}$  [18] and its effective mass  $m^* = 0.42m_e$  [19,20] is remarkable. Our results thus provide direct insight into how the  $s$ - $p$  derived Cu(111) surface state emerges from the coupling between  $sp_z$  hybrid adatom resonances.

The present findings imply several interesting consequences. First, they suggest that quasiatomic resonances associated with native adatoms as well as quantum confinement in assembled adatom structures do exist for various other one-component metal systems (i.e., the very systems known to exhibit surface states trapped in pseudogaps of the projected bulk band structure). Regarding the system studied here, our previous DFT calculations give also indication for the counterpart of the well known  $d$  band split-off Tamm state of Cu(111) [21]: apart from the unoccupied  $sp_z$  resonance, the calculations reveal the existence of occupied adatom [9] and chain-localized states [8] deriving from  $d$ -like atomic orbitals. The latter are more localized in character than the  $sp_z$ -derived state, reflecting the fact that split-off surface states are considered to be due to surface-induced changes in crystal potential while the formation of Shockley surface states implies an appreciable degree of delocalization to facilitate band crossing and opening of an inverted gap [22].

In conclusion, simple tight-binding modeling provides a clear-cut physical picture of electron confinement in surface-supported 2D structures consisting of only a few native adatoms. In the limit of large islands the well-known Cu(111) Shockley surface state emerges from the quantum states inherent to such structures which result from the coupling between  $sp_z$  hybrid adatom resonances. While various studies have shown that nearly-free-electronlike treatment is adequate to describe surface state scattering and confinement on the nanometer scale [18,23–27], TB [28] provides an instructive approach to explore how electronic properties evolve when building artificial surface structures atom by atom. A detailed understanding of such a scenario is an essential step towards the ultimate goal of “tailoring” magnetic and electronic surface properties by controlling size, geometry, and composition at the atomic level.

Support of this work by the European Union RTN network project *NANOSPECTRA* (Contract No. RTN2-2001-00311) is gratefully acknowledged.

- [1] W. A. de Heer, *Rev. Mod. Phys.* **65**, 611 (1993).
- [2] J. Bansmann *et al.*, *Surf. Sci. Rep.* **56**, 189 (2005).
- [3] U. Heiz and E. L. Bullock, *J. Mater. Chem.* **14**, 564 (2004).
- [4] D. M. Eigler and E. K. Schweizer, *Nature (London)* **344**, 524 (1990).
- [5] G. Meyer, S. Zöphel, and K. H. Rieder, *Phys. Rev. Lett.* **77**, 2113 (1996).
- [6] J. Tersoff and D. R. Hamann, *Phys. Rev. B* **31**, 805 (1985).
- [7] N. Nilius, T. M. Wallis, and W. Ho, *Science* **297**, 1853 (2002).
- [8] S. Fölsch, P. Hyldgaard, R. Koch, and K. H. Ploog, *Phys. Rev. Lett.* **92**, 56803 (2004).
- [9] F. E. Olsson, M. Persson, A. G. Borisov, J.-P. Gauyacq, J. Lagoute, and S. Fölsch, *Phys. Rev. Lett.* **93**, 206803 (2004).
- [10] S.-W. Hla, K.-F. Braun, V. Iancu, and A. Deshpande, *Nano Lett.* **4**, 1997 (2004).
- [11] J. Repp, G. Meyer, K.-H. Rieder, and P. Hyldgaard, *Phys. Rev. Lett.* **91**, 206102 (2003).
- [12] K. A. Fichtorn, M. L. Merrick, and M. Scheffler, *Phys. Rev. B* **68**, 041404(R) (2003).
- [13] N. V. Smith, *Phys. Rev. B* **32**, 3549 (1985).
- [14] The steady increase in  $dI/dV$  signal at high sample bias is due to the extension of the pseudogap and the onset of image states below the vacuum level [13].
- [15] P. Atkins and J. de Paula, *Physical Chemistry* (Oxford University Press, New York, 2005).
- [16] M. Persson, *Phys. Rev. B* **70**, 205420 (2004).
- [17] The observed resonance broadening estimated from the low-lying states decreases with island size and is  $\sim 0.8 \text{ eV}$  for  $\text{Cu}_3$ ,  $\sim 0.7 \text{ eV}$  for  $\text{Cu}_6$ , as well as  $\sim 0.6 \text{ eV}$  for  $\text{Cu}_{10}$  and  $\text{Cu}_{15}$ .
- [18] M. F. Crommie, C. P. Lutz, and D. M. Eigler, *Nature (London)* **363**, 524 (1993).
- [19] P. O. Gartland and B. J. Slagsvold, *Phys. Rev. B* **12**, 4047 (1975).
- [20] L. Bürgi, L. Petersen, H. Brune, and K. Kern, *Surf. Sci.* **447**, L157 (2000).
- [21] P. Heimann, J. Hermanson, M. Miosga, and H. Neddermeyer, *Phys. Rev. B* **20**, 3059 (1979).
- [22] S. G. Davison and M. Steslicka, *Basic Theory of Surface States* (Clarendon, Oxford, 1992).
- [23] E. J. Heller, M. F. Crommie, C. P. Lutz, and D. M. Eigler, *Nature (London)* **369**, 464 (1994).
- [24] L. Diekhöner, M. A. Schneider, A. N. Baranov, V. S. Stepanyuk, P. Bruno, and K. Kern, *Phys. Rev. Lett.* **90**, 236801 (2003).
- [25] J. Li, W.-D. Schneider, R. Berndt, and S. Crampin, *Phys. Rev. Lett.* **80**, 3332 (1998).
- [26] J. Li, W.-D. Schneider, S. Crampin, and R. Berndt, *Surf. Sci.* **422**, 95 (1999).
- [27] L. Bürgi, O. Jeandupeux, A. Hirstein, H. Brune, and K. Kern, *Phys. Rev. Lett.* **81**, 5370 (1998).
- [28] It is noted that TB modeling was also applied previously to describe surface state standing wave patterns on (111) noble metal surfaces in order to account for deviations in dispersion from free-electronlike behavior [20].